Interaction of Micrometeorites with Gaseous Targets

J C Slattery,* J F Friichtenicht,* and B Hamermesh*
Space Technology Laboratories, Inc , Redondo Beach, Calif

Experiments have been conducted on the interaction of simulated micrometeoroids with gaseous targets Iron spheres from 0 5 to 2 0 μ in diameter were accelerated to speeds up to 7 km/sec in the Space Technology Laboratories (STL) electrostatic accelerator Oxygen, argon, and air were used as target gases Gas pressures ranged from 1 to 2 mm Hg, which insured that conditions for free molecular flow were realized Values of the drag coefficient Γ and the heat-transfer coefficient λ were determined In this paper, λ is defined as the fraction of particle kinetic energy converted to internal energy and is applicable only for solid particles The results are consistent with a value of Γ nearly equal to one for all of the gases The values of λ depended upon the gas used and ranged from 0 8 to about 1 0

I Introduction

THE entry of a meteoroid into the earth's atmosphere is observable from the earth by visual and radar techniques Data from these observations are used to deduce physical parameters of the meteor and the upper atmosphere However, the mass and density of the meteoroid are unknown, and certain assumptions must be made concerning the physical constants involved For example, values must be assigned to the drag coefficient, the efficiency of energy transfer to the particle, the fraction of kinetic energy converted to light, and the efficiency for creating ion pairs A summary of the theory of meteoric processes and a discussion of existing data may be found in Ref 1 We are concerned in this paper with only the drag coefficient and the heat-transfer coefficient

Following the notation of Ref 1, we will review briefly the theory of meteors If a particle of mass m having a velocity v enters a region of the atmosphere having a density ρ, some of the momentum of the particle is transferred to the gas molecules, and the particle is decelerated according to

$$m(dv/dt) = -\Gamma A \rho v^2 \quad (1)$$

where Γ is the drag coefficient and A is the projected area of the particle

A second equation is obtained by considering the conservation of energy A fraction Λ of the energy of the particle is converted into heat, which manifests itself by raising the temperature of the body, melting, vaporization, or fragmentation In the general theory, it is assumed that the primary mechanism for energy dissipation is by vaporization of the meteoroid The particle collides with a mass of gas equal to $(\rho v A)$ per unit time, and, since the relative velocity of particle and gas molecule is v, we find

$$\zeta(dm/dt) = (\Lambda/2)A\rho v^3 \quad (2)$$

where ζ is the energy per unit mass required to vaporize the particle The kinetic energy lost by deceleration has been neglected in Eq (2), since this is negligible for naturally occurring meteoroids

The ablated atoms collide with gas molecules, and radiation is emitted Since an iron atom moving at a velocity of 22 km/sec has an energy of about 140 ev, it is clear that there is sufficient energy to excite and ionize the atoms of the meteoroid as well as the atoms in the atmosphere Meteor streams generally have velocities above 22 km/sec, and meteor spectra indicate that the excited atoms of the meteoroid emit most of the observed radiation

For the purposes of this paper, we will be concerned mainly with these two equations As will be described later, meteoroid processes can be studied in the laboratory under controlled conditions The experimental apparatus allows one to project artificial micrometeoroids having diameters the order of 1 μ and moving at speeds up to 8 km/sec into gas targets The composition and density of the target gas are known, and the parameters of the particles are specified

It is well to point out that there are certain differences between these experiments and the entry of a meteoroid into the earth's atmosphere The meteoroids that give rise to visible trails and radar echoes are much larger than the experimental particles Therefore, the thermal equilibrium time constant for our particles is much shorter In most respects this is a desirable characteristic for the kinds of measurements we have made since the phase (solid, liquid, or vapor) of the particle is more easily specified A further difference is that the change of velocity is not negligible, so in applying Eq (2) corrections must be made for the loss of kinetic energy due to deceleration In the general theory, Eq (2) is valid only for the case where the meteoroid is losing mass by ablation In fact, it is assumed that meteoroids are not observable until ablation occurs Most of our measurements, however, have been concerned with a determination of the heat-transfer coefficient while the particle is in the solid phase This quantity, denoted by λ, is defined in Sec IV Finally, the experimental particles are electrically charged This difference does not alter the basic measurements, but it does provide a very useful tool for following the particle and observing it as it undergoes changes of phase

In the experiments, simulated micrometeoroids were projected into various gases, and m, v, dv/dt, and charge loss were measured as functions of time Since the particles are very nearly spherical and their density is known, the value of A may be found Using an appropriate value of ζ with Eqs (1) and (2), values of Γ and λ were obtained In addition, the emission of light was observed as a function of time Although these last measurements can lead to values of luminous efficiency, only preliminary results of this type will be discussed

II Experimental Apparatus and Techniques

The STL electrostatic hypervelocity accelerator[2] was used as a source of high-speed particles for all of the measurements described in this paper In this accelerator, small particles are charged electrically by a process described elsewhere[3] and are injected into the accelerating field of a 2-Mv Van de

Presented as Preprint 63 462 at the AIAA Conference on Physics of Entry into Planetary Atmospheres, Cambridge, Mass , August 26–28, 1963; revision received January 3, 1964 This work was supported by NASA under Contract NASw-561

* Member Technical Staff

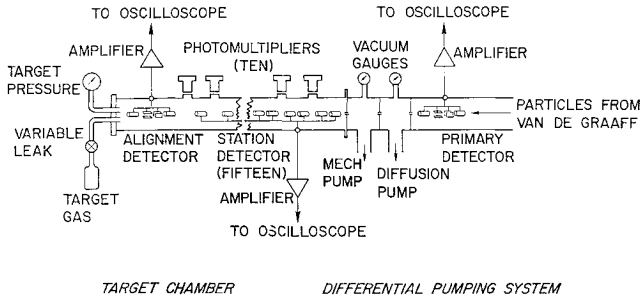

Fig 1 Schematic diagram of experiment

Graaff generator Here they are accelerated to a velocity given by

$$v = (2qV/m)^{1/2} \tag{3}$$

where V is the accelerating potential, m is the mass of the particle, and q is its charge As described in Ref 3, the q/m ratio obtainable is proportional to the reciprocal of the particle radius Consequently, the electrostatic method of accelerating particles is most effective for particles with small radii Under optimum conditions, a 1-μ-diam iron particle achieves a final velocity of about 7 km/sec Higher velocities can be obtained with particles of less dense materials For example, carbon particles have been accelerated to more than 20 km/sec For the experiments described here, only carbonyl iron spheres with an average diameter of about 1 5 μ were used

The charge and velocity of each particle issuing from the accelerator are determined by measuring the magnitude and duration, respectively, of a voltage signal induced on a cylindrical drift tube of known capacitance and length, through which the particles pass The charge is given by $q = CV_i$, where V_i is the magnitude of the induced voltage pulse and C is the capacitance of the drift tube to ground The velocity is simply $v = l/t$, where t is the time to pass through a cylinder of length l The mass (hence, the radius) of the particle is found from $m = 2qV/v^2$, where V is the accelerating voltage Generally, the signal on the drift tube is amplified and displayed on an oscilloscope trace, which is photographed for later analysis Detectors for determining particle position relative to the axis of the detector have also been developed These are described in Ref 3

The conditions for hypersonic free molecular flow for particles of this size range are satisfied for pressures of about 25 mm Hg or less Since the accelerator section is maintained at high vacuum, a transition region from high vacuum to the gas target is required This is accomplished by means of a differential pumping system illustrated schematically in Fig 1 Two intermediate pressure regions are provided Gas flow from one region to another is restricted by means of the constrictions shown in the figure The smallest constriction is 0 050 in in diameter and 0 60 in long With this system, pressures up to about 5 mm Hg can be maintained in the target section while maintaining a pressure of $2\ 0 \times 10^{-5}$ mm Hg in the accelerator section The conditions for free molecular flow are also satisfied at much lower pressures, but the energy loss per unit path length becomes so small that measurements of the effects are difficult For the sake of convenience, we have chosen to work at pressures of about 2 mm Hg The pressure in the target region is adjusted by the variable leak control, and the pressures in the various regions are monitored by appropriate gages In operation, particles from the accelerator pass through a charge-velocity detector and then through the series of constrictions into the target region The focusing properties of the accelerator are such that about 50% of the particles from the accelerator enter the target region

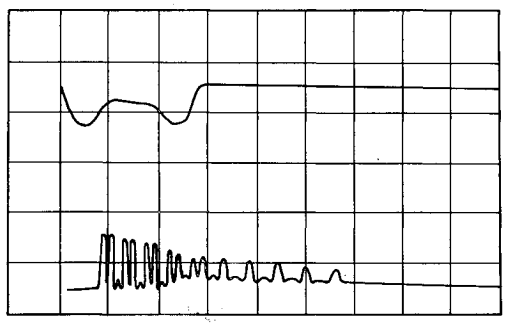

Fig 2 Typical oscilloscope trace The upper trace shows the output of the primary detector The vertical scale is 0 1 v/div, and the sweep speed is 5 0 μsec/div The lower trace shows the output of the 15-station detector The vertical scale is 0 1 v/div, and the sweep speed is 50 μsec/div

Two types of measurements were conducted during the course of this work One was concerned with the measurement of particle position and charge as a function of time This measurement made use of a series of 15 coaxial drift tubes (referred to as station detectors in Fig 1) interspersed with grounded drift tubes Each of the active drift tubes functions as a charge-velocity detector as previously described The detectors were connected in parallel and amplified by a common preamplifier

Preliminary measurements on radiant energy emission were made with the same target chamber Ten photomultipliers (RCA Type 7117 Multiplier Phototube with S-4 spectral response) were placed along the trajectory of the particle with a 3-in separation between tubes The signals from the phototubes were fed through cathode-follower amplifiers to an impedance-matching network where the outputs were added together The combined signals were then displayed on an oscilloscope The duration of the signal from each tube was short compared to the transit time between photomultipliers, so that a typical signal consisted of a series of ten (or fewer) discrete pulses The amplitude of each pulse was proportional to the radiant energy incident on the photocathode of the tube In the cases where fewer than ten pulses appeared, correlation was accomplished using time-of-flight techniques utilizing the time base generated by the primary detector The gains of the phototubes were adjusted periodically to a common, although arbitrary, value by means of a modulated tungsten filament light source

III Measurement of the Drag Coefficients

The velocity of a solid spherical particle traveling through a rarefied gas should obey the fundamental drag equation, derivable from Eq (1):

$$\frac{dv}{dt} = -\frac{\Gamma\rho\pi r^2}{m}v^2 \tag{4}$$

where ρ is the gas density, r and m are the particle radius and mass, v is the particle velocity, and Γ is the drag coefficient This equation may be integrated to give

$$\frac{1}{v} = \left[\frac{\Gamma\rho\pi r^2}{m}\right]t + \frac{1}{v_0} \tag{5}$$

The quantity in brackets is constant for a given particle Therefore, a graph of reciprocal velocity vs time should be a straight line with a slope directly proportional to the drag coefficient Experimentally, we measured distance vs time and computed the average velocity between points

The position measurement was accomplished with the 15-station detector previously described The detector signal was amplified by a calibrated preamplifier and presented on an oscilloscope with calibrated vertical amplifiers and sweep speeds A tracing of a typical oscilloscope pic

Table 1 Drag coefficients[a]

Oxygen data[b]			Argon data[c]			Air data[d]		
v_0, km/sec	r, μ	Γ	v_0, km/sec	r, μ	Γ	v_0, km/sec	r, μ	Γ
5 8	0 32	1 02	6 8	0 23	0 94	6 7	0 31	1 13
5 3	0 43	1 27	5 1	0 51	0 94	6 4	0 29	1 24
5 2	0 37	1 09	4 9	0 63	0 93	5 7	0 41	1 11
4 8	0 54	1 24	4 7	0 55	0 91	5 1	0 52	1 03
4 7	0 65	1 14	4 2	0 55	0 88	4 8	0 56	1 03
4 7	0 62	1 12	4 1	0 68	0 96	4 7	0 57	0 88
4 6	0 64	1 14	3 7	0 56	0 92	4 7	0 57	1 01
4 6	0 42	0 68	3 6	0 73	0 84	4 3	0 43	1 02
4 5	0 61	1 20	3 5	0 93	1 01	4 0	0 55	1 16
4 4	0 61	0 81	3 4	0 97	1 02	4 0	0 55	1 10
4 4	0 54	0 84	3 2	1 08	1 02			
4 4	0 42	0 86	2 8	1 11	1 12			
4 4	0 59	1 06						
4 3	0 68	1 06						
3 7	0 71	0 95						
3 4	1 02	1 23						
3 1	1 06	1 20						

[a] Mean values with rms deviations: $\Gamma_O = 1\ 05 \pm 0\ 17$; $\Gamma_A = 0\ 96 \pm 0\ 08$; and $\Gamma_i = 1\ 07 \pm 0\ 09$
[b] Gas pressure = 2 0 and 1.0 mm Hg
[c] Gas pressure = 1 3 mm Hg
[d] Gas pressure = 1 5 mm Hg

tune is shown in Fig 2 The upper trace is from the primary detector located just ahead of the differential pumping system, and the bottom trace is from the 15-station detector inside the gas

Each oscilloscope trace was measured with a traveling microscope, and a plot of reciprocal velocity vs time was made for each particle A typical plot is illustrated in Fig 3 The best straight-line fit for each set of points was found by a least-squares analysis A value of Γ was then computed using the particle parameters derived from the primary detector The gas pressure was measured with a calibrated thermocouple gage, corrected for the thermal conductivities of the different gases

The results of these measurements are presented in Table 1 The radius and initial velocity of each particle are included All the data were taken at gas pressures such that the molecular mean free path was large compared to the particle diameter, and the conditions for hypersonic free molecular flow were fulfilled

Although there is some spread in the data, we are led to the conclusion that the drag coefficient is very close to unity for iron particles and the three different gases used

IV Measurement of the Heat-Transfer Coefficient

In order to describe the energy transfer from the gas to the particle, we have followed the treatment normally used to describe meteoroid entry into the atmosphere The mass of gas striking the particle per unit time is $\rho\pi r^2 v$, where ρ is the gas density, πr^2 is the particle projected area, and v is the particle velocity The energy brought in by the gas is $\frac{1}{2}$ (mass) $\times$ (velocity)^2, and a fraction λ of this energy is converted into particle internal energy Thus, we have

$$dE/dt = (\lambda/2)\rho\pi r^2 v^3 \qquad (6)$$

where E is the internal energy of the particle We are defining the heat-transfer coefficient λ by the foregoing equation

If we could follow the temperature of a particle proceeding through the gas, the behavior would be somewhat as follows Along the first part of the path, all the energy is going into raising the temperature while radiation and vaporization losses are negligible When the temperature reaches 1535°C, the melting point, there is an interval of constant temperature during which the particle melts The thermal time constant for a spherical particle is of the order of $t \approx Cr^2\rho/k$, where C is the specific heat, k is the heat conductivity, ρ is the particle density, and r is the radius For a 1-μ diam iron particle, this time is about 2×10^{-8} sec Since the times involved in our experiments are of the order of tens of microseconds, we expect the particle to be at a substantially uniform temperature

Once the particle has melted, the temperature will start to rise again, since energy is still pouring in At some later time the energy lost by thermal radiation becomes important, and the temperature does not increase as rapidly However, the vast majority of our particles are fast enough so that they are temperature limited, not by radiation, but by vaporization The temperature climbs to something over 3000°K, where the energy lost by vaporization and radiation balances the input energy

The particle continues to slow down, and the energy being delivered decreases The temperature, limited by vaporization, also decreases Finally, a point is reached where there is little energy lost by vaporization, and the temperature is controlled by the thermal radiation The time constant for a particle losing energy by radiation alone is relatively long, and so the temperature falls more slowly At this point our experiments usually end

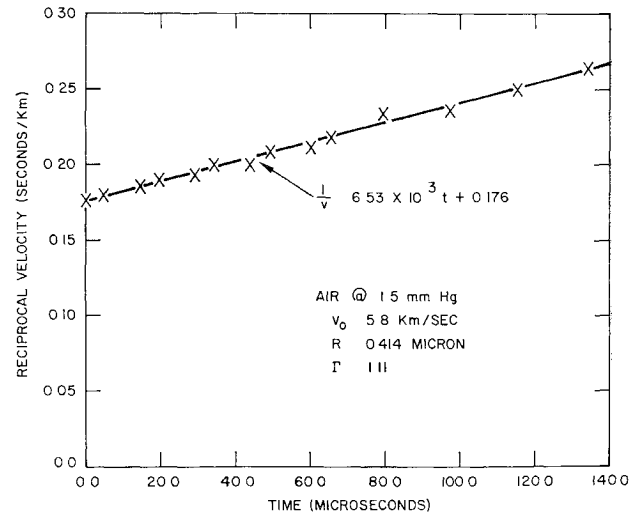

Fig 3 Least-squares fit of reciprocal velocity vs time for a typical particle

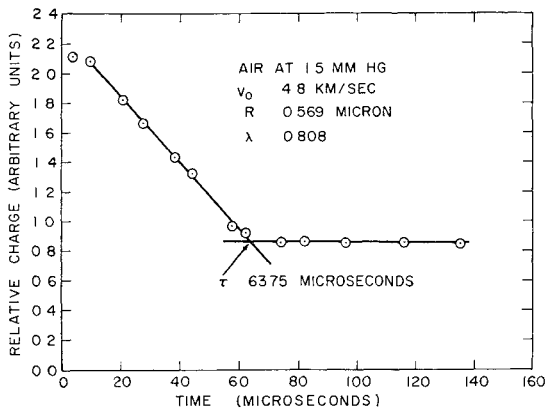

Fig 4 Graph of charge vs time for a typical particle illustrating the method used to find the time of melting

It is obvious that, if we could measure the temperature and mass ablation as a function of velocity, we could compute the heat-transfer coefficient However, the measurement of mass ablation at low velocities and with small particles is very difficult Without knowing how much energy is going into vaporization, it would be of little use to know how much goes into radiation

On the other hand, there is a section of the particle track where we may be relatively certain that little energy is going into either vaporization or radiation This is the time interval just after the particle has entered the gas All the energy is being used to raise the particle temperature toward the melting point We need only to identify the melting point at 1535°C, and we may calculate directly the heat transferred to the particle

We believe that the behavior of the charge on the particle gives an indication of when the particle turns molten

All particles, without exception, lose some fraction of their charge shortly after entering a gas target This applies to all the gases we have used In general, the charge follows a curve very similar to those illustrated in Figs 4 and 5 There seems to be a short time when the charge loss is small, and then an almost linear decrease occurs Invariably, the loss then stops, and the particle continues on with a constant charge If the curve is followed further, the charge once again starts to decrease as illustrated in Fig 5 and, in a time comparable to the first decrease, goes to zero

The explanation we advance for this behavior is as follows When the particles first enter the gas, the average electric field at the surface is 2×10^9 v/m Small irregularities on the surface enhance this field at local spots The combination of high fields and bombardment by gas atoms with an energy equivalent to a few electron volts causes the emission of ions We do not know whether the ions emitted are iron, iron oxides, or ionized target gas However, a combination of gas and field is necessary since there is no charge loss for a particle traveling through vacuum

Whatever the actual mechanism of initial charge loss, the critical assumption we make is that the melting of the particle smooths out the local irregularities and lowers the field At this point the charge emission stops We take the knee of this curve to be the time of melting and measure it as indicated in Figs 4 and 5 A graph of charge vs time was made for each particle analyzed, and the time the particle melted was determined in this manner

Since we are dealing with highly charged solid spheres that become molten, it is of interest to calculate the Rayleigh limit[4] of our particles; namely, that value of the charge q on a liquid droplet of radius r at which the coulomb repulsion just balances the force due to surface tension α, i e , $q^2 = 64\pi^2\sigma\epsilon_0 r^3$ When the charge is below this limit, a liquid drop is stable against breakup Figure 6, illustrating some of the data for particles in air, shows that, although nearly all of our particles start with an amount of charge in excess of the Rayleigh limit, they fall below the limit before they reach the point where we assume they are molten The crosses in Fig 6 represent the initial particle charge, and the circles represent the charge on the same particle after it has ceased losing charge

There is still one uncertainty, and that is whether the latent heat of melting should be included If the particle melts from the surface, uniformly inward, probably little of the latent heat should be included, and only the energy necessary to raise the temperature by 1500°K would be counted Since the heat is delivered on the front side only, perhaps an acceptable compromise would include only one-half of the latent heat of melting The analysis of the data does not include the latent heat, but it is a simple matter to correct the results so as to take this into account

To find λ, we equate the energy necessary to raise the particle temperature by 1500°K to the energy delivered over a time τ,

$$mC(1500) = \int_0^\tau \frac{\lambda}{2} \rho\pi r^2 v^3 dt \qquad (7)$$

We chose an average specific heat C of 0 165 cal/g-°C for iron over this temperature range The particle mass m was measured as described in Sec II, and the particle radius was

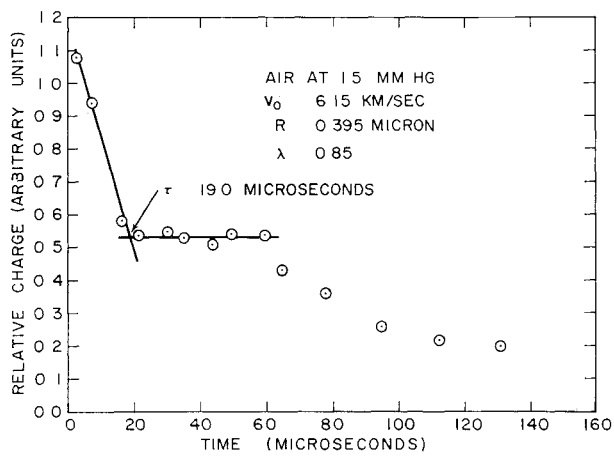

Fig 5 Graph of charge vs time for a particle that displays loss of charge during latter part of trajectory

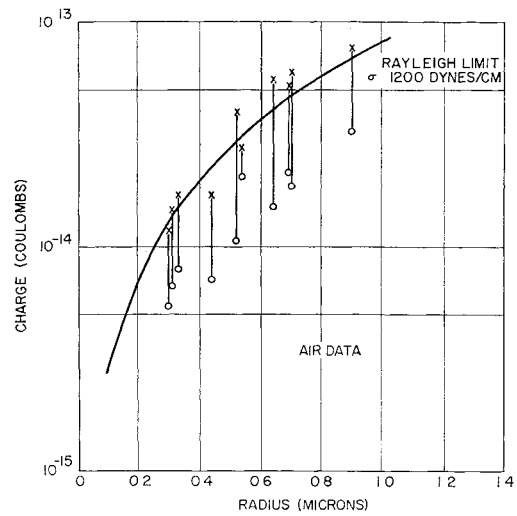

Fig 6 The solid curve is the Rayleigh limit (see text) for liquid particles with a surface tension of σ = 1200 dyne/cm Each cross and open circle represents one experimental particle The cross represents the initial charge, and the open circle represents the charge after the particle has melted

Table 2 Heat-transfer coefficients[a]

Oxygen data[b]			Argon data			Air data[d]		
v_0 km/sec	r μ	λ	v_0, km/sec	r, μ	λ	v_0, km/sec	r, μ	λ
4 2	0 66	1 07	5 0	0 51	0 98	6 7	0 31	0 89
4 1	0 65	1 05	4 9	0 63	0 79	6 5	0 30	0 76
4 0	0 81	1 00	4 7	0 55	0 94	6 2	0 40	0 84
3 7	0 67	1 09	4 6	0 58	0 99	6 0	0 46	0 80
3 6	0 87	1 07	4 2	0 71	0 84	5 2	0 63	0 81
3 6	0 96	1 08	4 2	0 55	0 97	4 8	0 57	0 81
3 4	1 00	0 99	4 0	0 84	0 96	4 7	0 57	0 94
3 4	0 64	1 06	3 8	0 56	0 86	4 6	0 66	0 97
3 3	0 60	1 05	3 7	0 85	0 96	4 4	0 63	0 83
3 2	0 66	1 09	3 6	0 70	0 75	4 4	0 43	0 78
						4 0	0 55	0 99
						3 9	0 71	0 88
						3 8	0 70	0 91

[a] Mean values with rms deviations: $\lambda_O = 1\ 06 \pm 0\ 03$; $\lambda_A = 0\ 90 \pm 0\ 08$; and $\lambda_i = 0\ 86 \pm 0\ 07$ For nitrogen (obtained by combining air and oxygen data) $\lambda_N = 0\ 81 \pm 0\ 09$.
[b] Gas pressure = 2 0 mm Hg
[c] Gas pressure = 1 3 mm Hg
[d] Gas pressure = 1 5 mm Hg

derived from $m = \frac{4}{3}\pi r^3 \rho_F$, with the density of iron taken as 7 8 g/cm^3 The gas density ρ was derived from the pressure measured by a calibrated thermocouple gage The reciprocal velocity was plotted vs time for each particle, as illustrated in Fig 3, and the measured curve was used to determine the velocity function used in the integral The measured heat-transfer coefficients are presented in Table 2, along with the initial velocities and particle radii The heat-transfer coefficient for nitrogen was calculated from those of oxygen and air by the following equation:

$$\lambda_{air} = 0\ 79\lambda_{N_2} + 0\ 21\lambda_{O_2} \qquad (8)$$

Since the latent heat of melting is not included, these values would represent a lower limit Inclusion of the latent heat would mean raising all the values of λ by a factor of $(1 + L/1500C)$, where L is the latent heat of melting and C is the specific heat If we take $L = 64$ cal/g and $C = 0\ 165$ cal/g-°C, this factor is 1 26 Should only one-half of the latent heat be used, then the correction factor is 1 13

There is one other correction that should be applied to the heat-transfer coefficient derived for oxygen This would take into account the possible addition of chemical energy from the exothermic reaction of iron and oxygen The fact that the oxygen data consistently yield coefficients greater than unity indicates that something of this nature is taking place At natural meteor velocities the relative contribution of this chemical energy will be much smaller, since the kinetic energy contribution increases as the square of the velocity

Accounting for this energy is difficult, but if we assume that the heat-transfer coefficient for oxygen is the same as the average of argon and air, then the difference between measured and assumed values would be due to chemical reactions With this assumption, we can calculate the average chemical energy delivered per molecule of oxygen striking the particle When this has been done, we find that the average energy is 0 35 ev/molecule Since iron-oxygen reactions have typical energies of 2 or 3 ev, this result implies that about one out of ten molecules that strike the particle reacts chemically

At the present time we have no direct evidence to support the assumption that the particle reaches the melting point coincident with the cessation of charge loss However, the results are consistent with this assumption, and there are several points that argue in favor of this conclusion

In the first place, the heat-transfer coefficients are close enough to unity that melting cannot occur much earlier than we designate This would require energy transfer with an efficiency greater than 100% Melting must then occur either at the time we indicate or sometime later If it is later, then an argument must be developed to explain the cessation of charge loss without a change of phase Examination of the data indicates that the melting argument is consistent with the observations although other explanations are not For example, the effect is not directly related to the electric field since the field varies by at least a factor of two between particles It is not a function of the time spent by the particle in the gaseous environment because this varies by an order of magnitude Charge loss does not cease at a given particle velocity The results, however, are consistent with a temperature rise; i e , they obey Eq (7) reasonably well as shown in Table 2

Further support for the melting hypothesis is obtained from the results of a separate set of experiments In these experiments, photomultiplier tubes were interspersed with the charge detectors along the gas target tube Thus, we observed the charge loss and light emission simultaneously The visible light emitted by the particle was observed to rise sharply to a maximum along the trajectory and then decay The maximum occurs later than the knee on the charge curve

In Fig 7 we have taken one particle and plotted the measured velocity and light output vs time By assuming a heat-transfer coefficient of unity and knowing the particle

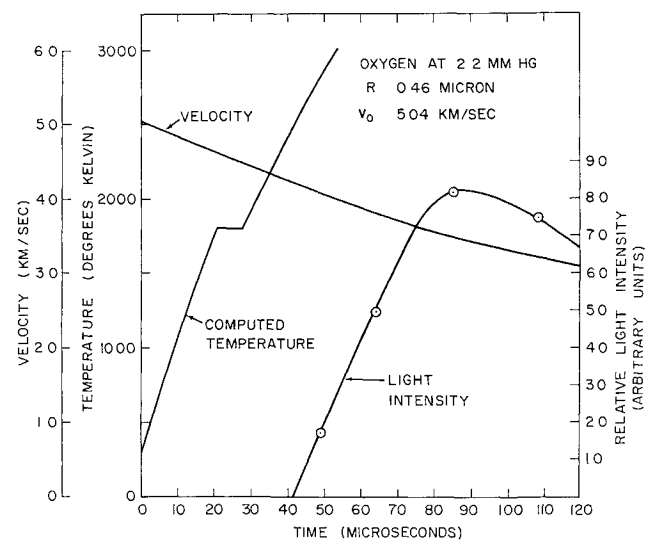

Fig 7 Graph illustrating measured velocity and measured light output for a typical particle Included is a plot of particle temperature computed assuming a heat-transfer coefficient of unity (see text for a more complete discussion)

mass and velocity, we may compute the temperature rise of the particle The results of this calculation are included in Fig 7 also The actual temperature will rise less sharply above 2000°K than indicated because we have neglected any energy losses by radiation in the computed curve

The calculated thermal time constant of a particle losing energy by radiation alone is much longer than the observed decrease in the light output Fiom this we infer that vaporization is limiting the particle temperature near the peak of the light output curve If this is the case, the temperature must be in the neighborhood of 3000°K or higher We may then look back along the particle trail and estimate when the temperature was 1800°K When this is done, the results agree with our original assumption that the particle is near 1800°K when the charge loss stops

V Summary

The drag coefficients of small spherical paiticles traveling through oxygen, argon, and air under conditions of hypersonic free molecular flow have been measured The results presented in Table 1 are consistent with a value of unity for the drag coefficient in all three gases The measurement technique was straightforward, and the deviations in the results can probably be ascribed to experimental errors on individual particles

We have derived a value for the heat-transfer coefficients in the same three gases and under the same conditions In order to calculate these coefficients we found it necessary to make certain assumptions concerning the temperature and physical state of the particles These assumptions are outlined in Sec IV None of these arguments is conclusive proof, but they are all consistent We conclude, therefore, that the values of heat-transfer coefficients, which we have tabulated in Table 2, are valid lower limits for this velocity and particle regime

References

[1] Whipple, F L and Hawkins, G S , ' Meteors,'' *Handbuch der Physik* (Springer-Verlag, Berlin, 1959), Vol III

[2] Friichtenicht, J F , Rev Sci Instr **33,** 209–212 (1962)

[3] Shelton, H , Hendricks, C D , Jr , and Wuerker, R F , J Appl Phys **31,** 1243–1246 (1960)

[4] Rayleigh, J W S , Phil Mag **5,** 14, 184 (1882); also *The Theory of Sound* (Dover Publications, Inc , New York, 1945), Vol II, p 372